Proceedings of the Korean Nuclear Society Spring Meeting, Kori, Korea, May 2000

Direct-contact Condensation Experiments for the Stratified Liquid Flow with Steam and Steam/Air mixture in a Circular Pipe

Sung Won CHOI[1], Hyun Sik PARK[2], Hee Cheon NO[1], and Young Seok BANG[3]

[1] Korea Advanced Institute of Science and Technology
373-1 Kusong-Dong, Yusong-Gu, Taejon, 305-701, Korea

[2] Korea Atomic Energy Research Institute
150 Dukjin-Dong Yusong-Gu, Taejon, 305-353, Korea

[3] Korea Institute of Nuclear Safety
19 Kusong-Dong Yusong-Gu, Taejon, 305-338, Korea

Abstract

Direct-contact condensation experiments of atmospheric steam and steam/air mixture on sub-cooled water flowing co-currently and counter-currently are carried out in a circular pipe. The condensation heat transfer was evaluated in counter-current flow in a horizontal circular pipe with steam-water or steam/air mixture-water flow, and in co-current flow with steam-water flow. The experimental results show that logarithmic heat transfer coefficients increase as the inlet liquid Reynolds number increases and the inlet steam Reynolds number increases, but it decreases as the inlet air mass fraction increases. Empirical correlations for liquid Nusselt number are developed for both co-current and counter-current flows, and their predictions are compared to show good agreements with the experimental data.

1. INTRODUCTION

Direct contact condensation is fundamentally important in LWR (Light Water Reactor) safety analysis and other industrial applications. Especially, during a postulated LOCA (Loss of Coolant Accidents), cold ECCW (Emergency Core Cooling Water) would be injected to cool down the reactor core. When the subcooled water is injected into the horizontal pipe filled with steam, the steam flows over the water in the opposite direction and steam condensation occurs in a stratified flow. The local condensation rate and the relative motion of steam and water are important in the determination of core uncovery. Furthermore the local condensation heat transfer coefficients are the key parameter of water hammer. Because the system behavior for these case is highly dependent upon the local condensation rate.

There have been a lot of theoretical and experimental research on horizontal in-tube condensation using a rectangular channel which has large aspect ratio and thin water layer thickness. However, it must be doubtful whether existing correlations obtained by rectangular channel can evaluate the nuclear piping systems directly.

The objectives of present studies are to evaluate the condensation heat transfer and develop empirical correlations both in co-current flow with steam-water flow and in counter-current flow with steam-water flow and steam/air mixture-water flow in a horizontal circular pipe to be compared with each other, and to investigate effects of several parameters such as the sub-cooled inlet water temperature, the gas mixture and water flow rate and the air mass fraction.

2. EXPERIMENTAL WORKS

2.1 Description of an Experimental Loop

An adiabatic two-phase loop is modified to carry out direct-contact condensation experiments. The overall schematic diagram of the experimental facility is shown in Figure 1. The main component of experimental facilities are consisted of water, steam supply system, test section and data acquisition systems. Steam supplied by 100kw steam generator passes through two steam-water separators and then it is injected into the test section. The temperature in the steam generator is maintained about 130℃ during the experiment to compensate the loss of heat in a long pipeline. Steam which is controled by control valve can be mixed with heated air before passing through steam-water separator for the experiment to investigate the non-condensable effects in condensation. The inlet water temperature is controlled by a heater and a heat exchange tank installed in a water supply tank.

Several variables are measured to obtain a direct-contact condensation heat transfer coefficient. In the test loop, the flow rate, pressure, and temperature of mixture layer in the test section are locally measured. The inlet pressure and temperature in the test section are measured at the top of the water vessel connected to the test section. Water subcooling is controlled based on the temperature measured in the water vessel. Inside the test section, local bulk mean temperatures are measured by using thermocouples and pitot tubes at three locations. As shown in Figure 2, K-type thermocouples with the outer diameter of 0.5 mm are attached to the side of pitot tube with the outer diameter of 1.5 mm with magic bond in order to move and measure the local tempeature and velocity at the same time.

2.2 Test Matrix and Experimental Procedure

The controllable test parameters are summarized in Figure 3 and the present test matrix is also shown in Table 1. The criteria of selecting test parameters and setting test matrix are

divided into two reasons. One is to estimate the suitability of appling the information obtained by rectangular channel experiments to the pipe system. The other is to examine effects of several parameters such as the sub-cooled inlet water temperature, the gas mixture and water flow rate and the air mass fraction.

The present experimental work is conducted through the following procedure:

1. Select the test type.
2. Control the inlet water temperature.
3. Fix the inlet water flow rate.
4. Measure the water layer thickness.
5. Increase the inlet steam flow rate.
6. Wait until the stable and saturated state.
7. Measure the temperature and velocity at three local positions.
8. Save the data.

3. DATA REDUCTION METHOD

3.1 Calculations of Water Bulk Temperature

The local water bulk temperature is defined as follows:

$$T_{f,bulk}(Z) = \frac{\int \rho_L(x,y,z)\, T_L(x,y,z)\ V_L(x,y,z) \cdot dx\, dy}{\int \rho_L(x,y,z)\ V_L(x,y,z) \cdot dx\, dy} \tag{1}$$

In order to evaluate the bulk temperature, as shown in Figure 4, the nodalization of water layer is divided by the height y. Local water temperature is calculated by summarizing each temperature and velocity value at certain height in water layer. The bulk liquid temperature can be calculated as follow:

$$T_{L,bulk}(z) = \frac{\sum_{j=1}^{n} T_{mean}(y_j,z)\, V_{mean}(y_j,z)\, S_i(y_j)\, \Delta y}{\sum_{j=1}^{n} V_{mean}(y_j,z)\, S_i(y_j)\, \Delta y} \tag{2}$$

3.2 Local Heat Transfer Coefficient

To evaluate the averaged values of temperature and velocity at each vertical position from the bottom, the temperature and velocity profiles in the cross-sectionally horizontal direction are assumed as follows:

1. The temperature profile is uniform in the cross-sectionally horizontal direction from the results of Chun et al.(1999).

2. The velocity profile follows the 1/7 power velocity profile in the cross-sectionally horizontal direction.

3. The properties of steam along the test section are constant.

4. The heat transfer from steam and water side wall to the atmosphere is negligible. Actually it was shown that the steam condensation rate at the pipe wall is much less than the total steam condensation rate at the steam-water interface from the result of Chun et al.(1999).

From the energy balance equation, the heat transfer coefficient is defined as follow:

$$h_z = \frac{C_{pL} \cdot W_L(z)}{b[T_G - T_L(z)]} \cdot \frac{dT_L(z)}{dz} \quad . \tag{3}$$

Since $W_L(z)$ is also a function of $T_L(z)$, the local heat transfer coefficient can be determined only from $T_L(z)$ using the slope of liquid temperature, liquid flow rate, etc. The definition of dimensionless parameters in the present work are as follows:

$$\begin{aligned} Nu &= \frac{h_c D_{h,f}}{k_f} \quad , \qquad Re_k = \frac{\rho_k V_k D_{h,k}}{\mu_k} , \qquad k = f, g \ , \\ \Pr &= \frac{c_{p,f}\mu_f}{k_f} \quad , \qquad D_{h,f} = \frac{\pi D \cdot \alpha_f}{\pi - \alpha + \sin\theta} \quad . \end{aligned} \tag{4}$$

3.3 Log-Mean Heat Transfer Coefficient

The log-mean heat transfer coefficient, h_{log}, can be obtained from the total heat transfer area and the measured liquid and mixture temperatures both at the inlet and outlet as follow:

$$h_{\log} = \frac{Q_{total}}{A \cdot \Delta T_{\log}} \quad , \tag{5}$$

where A is the total heat transfer area and both ΔT_{log} and Q_{total} are the log mean temperature difference and the total heat flux from inlet to outlet, respectively. The log mean temperature difference is defined by

$$\Delta T_{\log} = \frac{\Delta T_1 - \Delta T_2}{\ln(\Delta T_1 / \Delta T_2)} \quad , \tag{6}$$

where

$$\Delta T_1 = T_{g,in} - T_{f,in} \ , \tag{7}$$

and

$$\Delta T_2 = T_{g,out} - T_{f,out} \quad , \tag{8}$$

where $T_{g,in}$, $T_{g,out}$, $T_{f,in}$, $T_{f,out}$ are temperatures of mixture and liquid both at the inlet and outlet.

3.4 Uncertainty Analysis

The uncertainty analysis for the local heat transfer coefficients has been carried out by an error propagation method.

$$\sigma^2(u) = \left(\frac{\partial u}{\partial x}\right)^2 \sigma^2(x) + \left(\frac{\partial u}{\partial y}\right)^2 \sigma^2(y) + \left(\frac{\partial u}{\partial z}\right)^2 + \ldots \quad (9)$$

The uncertainty of interfacial heat transfer coefficients, σ_h, is computed by root-sum-square method of bias limit, σ_B, and precision limit, σ_p, as follow:

$$\sigma_h = \sqrt{\sigma_B^2 + \sigma_p^2} \quad (10)$$

The maximum uncertainty of the interfacial condensation heat transfer coefficients is 27%, which is mainly due to the error of water bulk temperature that results from the error produced in the determination of water layer thickness. The detailed information are summarized in Table 2.

4. RESULTS AND DISCUSSION

4.1 Flow Regime

Experimental data are plotted on the Mandhane et al.(1974)'s flow pattern map to identify flow regimes of both co-current and counter-current gas-liquid flows in horizontal pipes as shown in Figure 6. The present experimental conditions of co-current flow lie in the stratified flow and wavy flow regimes and those of counter-current flow lie in the wavy flow and at the interface between wavy flow and slug flow regimes. Both flow rates of gas and liquid are much higher in co-current flow experiments than in counter-current flow experiments, and their predictions of flow regimes are identical with visual observations.

4.2 Co-Current Stratified Flow Experiments

12 sets of co-current direct-contact condensation experiments using pure steam are performed. Logarithmic heat transfer coefficients are calculated for pure steam data. Figure 7 shows the effect of the inlet steam Reynolds number on the heat transfer, in which the inlet liquid Reynolds number is used as a parameter. The logarithmic heat transfer coefficient increases with an increase in inlet steam Reynolds numbers and it also increases slightly with an increase in inlet liquid Reynolds numbers.

The experimental Nusselt number is correlated with the parameters of Re_f, Re_g, and Pr_f where the exponent of Pr_f is fixed to 0.95. Using the least-square method, the final correlation is expressed as follow:

$$Nu_f = 8.36 * 10^{-6} Re_f^{1.49} Re_g^{0.09} Pr_f^{0.95}, \quad (11)$$

which is applicable in the following operating ranges:

$$14766 < Re_f < 29559, \quad (12)$$

$$2486 < Re_g < 23655, \quad (13)$$

and

$$2.18 < Pr_f < 2.88 \ . \tag{14}$$

Equation (11) shows that the Nusselt number is much higher with an increase in the liquid Reynolds number Re_f. However, its dependency on Re_g is small.

Figure 8 shows the comparison of Nusselt numbers estimated from the experimental data with those calculated from the present correlation and four existing correlations. The standard deviation of the predictions of the present correlation from the experimental heat transfer coefficients is 15.8%. The Kim(1983)'s correlation with Froude number overestimates the experimental Nusselt numbers with standard deviation of 179.2%, and the other three correlations of Chun et al.(1999)'s, Segev et al.(1981)'s, and Kim(1983)'s with Reynolds number deviate with standard deviations of 50.0%, 32.8%, and 41.7%, respectively.

The correlations obtained by Segev et al.(1981) and Kim(1983) are based on a rectangular flow channel and a very shallow water layer thickness. However, the correlation obtained by Chun et al.(1999) are based on a circular flow channel and its prediction over the present experimental data is comparatively accurate.

4.3 Counter-Current Stratified Flow Experiments

12 sets of counter-current direct-contact condensation experiments using pure steam are performed and 24 sets are also performed using air/steam mixture. Figure 9 shows the effect of the inlet liquid Reynolds number on the heat transfer, in which the inlet mixture Reynolds number is used as a parameter. Similarly with experimental results of co-current flow, the logarithmic heat transfer coefficient increases slightly with an increase in inlet liquid Reynolds numbers and it also increases with an increase in inlet mixture Reynolds numbers.

Figure 10 shows the effect of the inlet air mass fraction on the heat transfer, in which the inlet liquid temperature is used as a parameter to show its degree of sub-cooling. The inlet air mass fraction changes between 0, 10, and 30%. The logarithmic heat transfer coefficient is much higher with pure steam than with steam/air mixture, but the difference of heat transfer coefficients between experiments with 10% and 30% air mass fractions is very small. The dependency of logarithmic heat transfer coefficient on the degree of subcooling is higher with pure steam, but it is very low with steam/air mixture.

Using similar approaches of co-current flow experiments, the experimental Nusselt number is also correlated with the parameters of Re_f, Re_g, and Pr_f, and the final correlation is expressed as follow:

$$Nu_f = 3.26 * 10^{-6} Re_f^{1.43} Re_g^{0.22} Pr_f^{0.95}, \tag{15}$$

which is applicable in the following operating ranges:

$$4573 < Re_f < 9350 \ , \tag{16}$$

$$4005 < Re_g < 13351 \ , \tag{17}$$

and

$$2.95 < Pr_f < 3.71 . \quad (18)$$

Equation (15) shows that the Nusselt number is much higher with an increase in the liquid Reynolds number Re_f. Especially, its dependency on Re_g increases compared more than that of co-current flow experiments.

Figure 11 shows the comparison of Nusselt numbers estimated from the experimental data with those calculated from the present correlation and four existing correlations. The standard deviation of the predictions of the present correlation from the experimental heat transfer coefficients is 11.6%. The Kim(1983)'s correlation with Froude number overestimates the experimental Nusselt numbers with standard deviation of 185.5%, and the other three correlations of Chun et al.(1999)'s, Segev et al.(1981)'s, and Kim(1983)'s with Reynolds number deviate with standard deviations of 18.5%, 24.0%, and 26.2%, respectively.

5. CONCLUSIONS

Several experiments are performed to obtain reliable data on the interfacial condensation phenomena to show the parametric effects on the condensation heat transfer and to develop an empirical correlations for both co-current and counter-current flows.

From the aforementioned studies, the following conclusions have been reached:

1. The logarithmic heat transfer coefficients increase as the inlet liquid Reynolds number increases and the inlet steam Reynolds number increases, but it decreases as the inlet air mass fraction increases.

2. Empirical correlations for liquid Nusselt number are developed for both co-current and counter-current flows. Their predictions are compared with the experimental data to show good agreement with standard deviations of 15.8% and 11.6% for both co-current and counter-current flows. Comparisons of the present experimental data with four existing correlations of Segev et al.(1981), Kim(1983), and Chun et al.(1999) showed that the Kim(1983)'s correlation with Froude number shows a much higher prediction than the experimentally estimated Nusselt number, and correlations of Segev et al.(1981)'s and Kim(1983)'s with Reynolds number does not predict well the experimental data with high standard deviations.

3. Developed empirical correlations show that dependency of liquid Nusselt number on Re_g are higher with counter-current experimental data than with co-current experimental data.

Acknowledgement

The authors gratefully acknowledge the financial support of Korea Institute of Nuclear Safety (KINS) provided for this work.

References

[1] Choi, K.Y., "Direct-contact condensation heat transfer with noncondensable gases and interfacial shear for co-current stratified wavy flow in nearly-horizontal channels," PhD. thesis, KAIST, 1998.

[2] Kim, H.J., "Local properties of countercurrent stratified steam-water flow," PhD. thesis, Northwestern Univ. Evanston, Illinois, 1983.

[3] Chun, M.H., Chu, I.C., and Yu, S.O., "Interfacial Condensation Heat Transfer for Countercurrent Steam-Water Stratified Flow in a Circular pipe," Ninth International Topical Meeting on Nuclear Reactor Thermal Hydraulics (NURETH-9), San Francisco, California, October 3-8, 1999.

[4] Mandhane, J.M., Gregory, G.A., and Aziz, K., "A flow pattern map for gas-liquid flow in horizontal pipes," Int. J. Multiphase Flow, Vol.1, pp.537-553, 1974.

[5] Segev, A., Flanigan, L.J., Kurth, R.E., and Collier, R.P., "Experimental study of counter-current steam condensation," J. Heat Transfer Trans. ASME, Vol.113, pp.307-311, 1981.

Table 1. Test matrix of the present experiments

Air Mass Fraction	Inlet Water Temperature (℃)	Inlet Water Flow Rate (gpm)	Inlet Steam Flow Rate (kg/hr)	Flow Regime
0	63	2	21 59	Inclined steam-water co-current flow
	63	4	19.3 59.2	
	52, 56	6	19.3, 24.6	
0	40	1.3, 1.9, 2.4	13.6, 21.6	Steam-water counter-current flow
	50	1.3, 1.9, 2.4	13.6, 21.6, 43	
0.1	40	1.3, 1.9, 2.4	13.6, 21.6	Air/steam mixture-water counter-current flow
	50	1.3, 1.9, 2.4	13.6, 21.6	
0.3	40	1.3, 1.9, 2.4	13.6, 21.6	
	50	1.3, 1.9, 2.4	13.6, 21.6	

Table 2. Uncertainty of local heat transfer coefficient

Parameter		Precision Limit	Bias Limit
Independent Parameter	Water layer thickness	0.005m	0.001m
	Inlet water flow rate	2%	1%
	Inlet steam flow rate	5%	1%
	Local water velocity	5%	5%
	Local water & steam temperature	0.5℃	1.2℃
Local heat transfer coefficient, h		24.4%	12.8%
Maximum uncertainty of local heat transfer coefficient, h		27.5%	

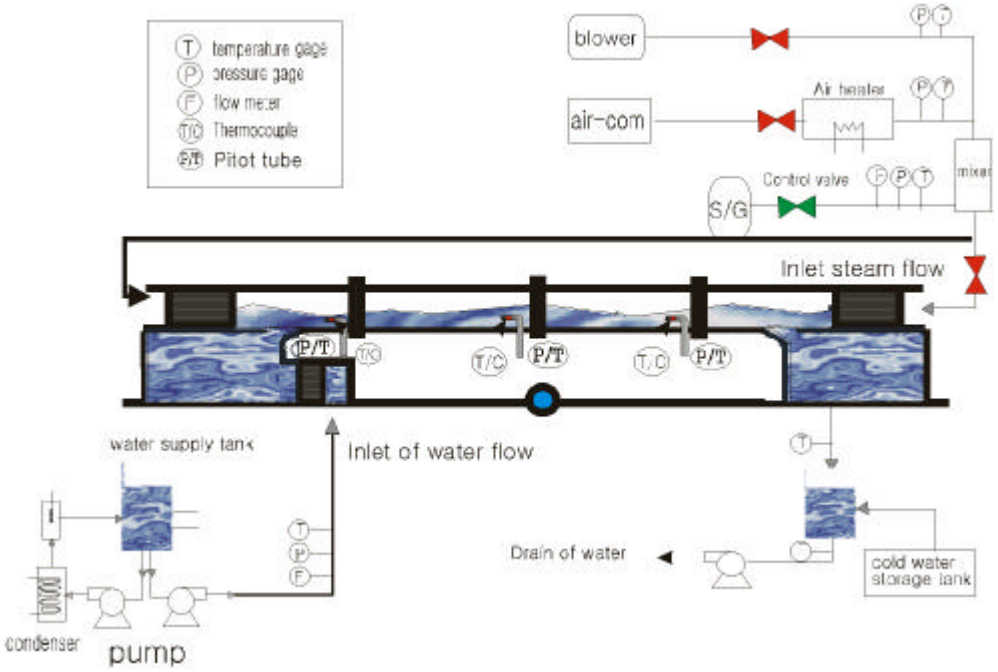

Figure 1. Schematic Diagram of the Experimental Apparatus

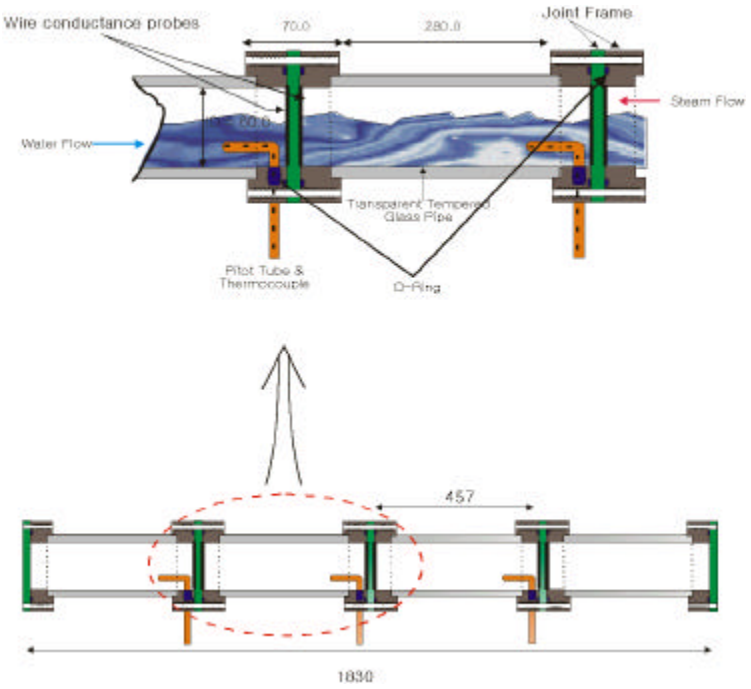

Figure 2. Temperature and velocity measurement system

Figure 3. Experimental procedure

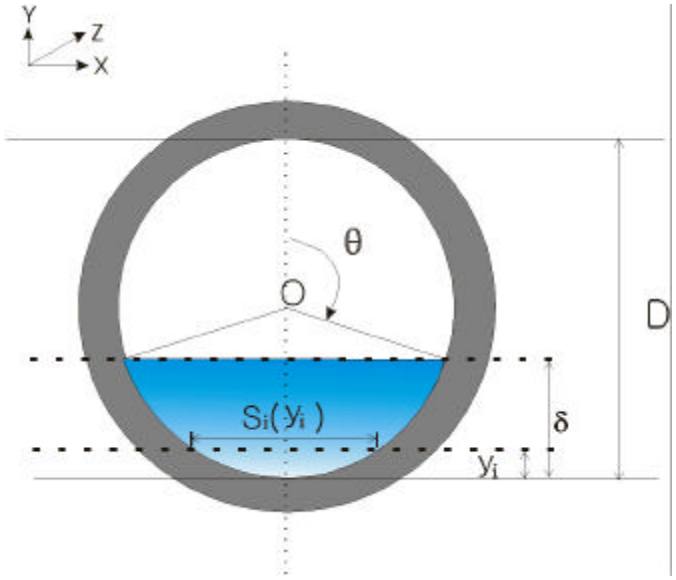

Figure 4. Nodalization for the calculation of water bulk temperature

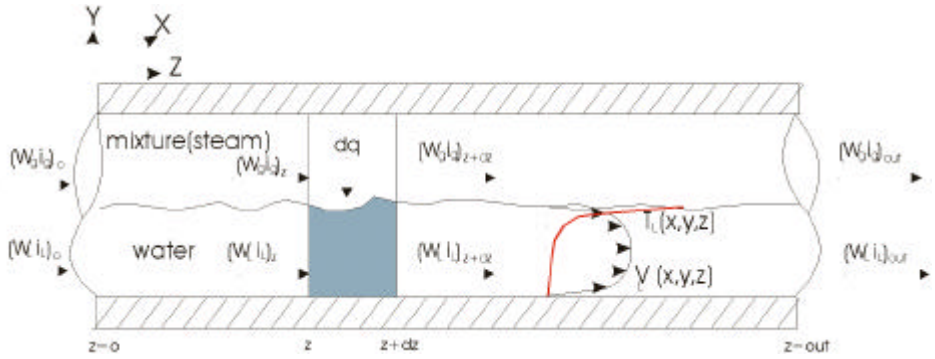

Figure 5. Energy balance in control volume

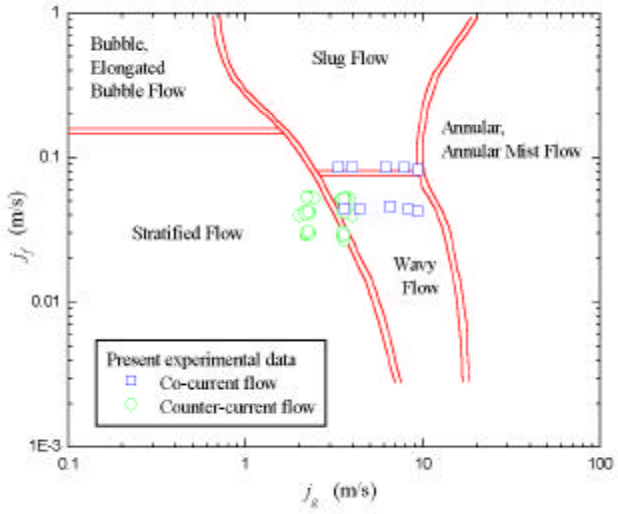

Figure 6. Experimental data plotted on the Mandhane et al.(1974)'s flow pattern map

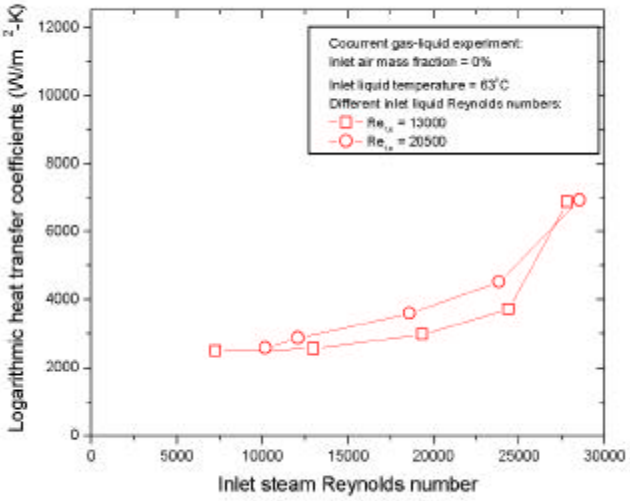

Figure 7. Effect of the inlet steam Reynolds number on logarithmic heat transfer coefficient

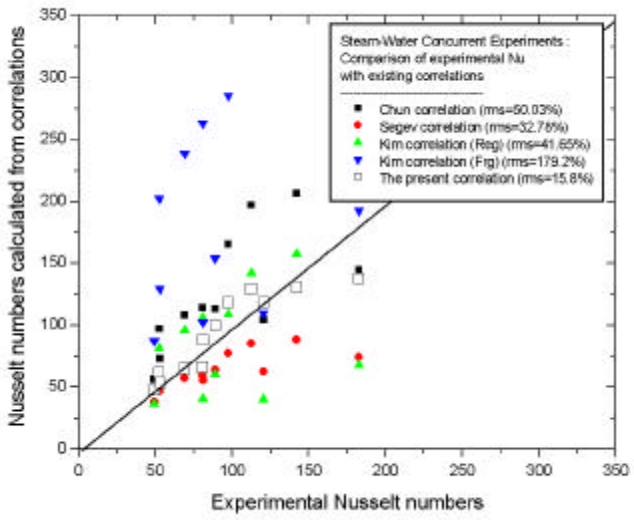

Figure 8. Comparison of Nusselt numbers estimated from the experimental data with those calculated from the present correlation and four existing correlations

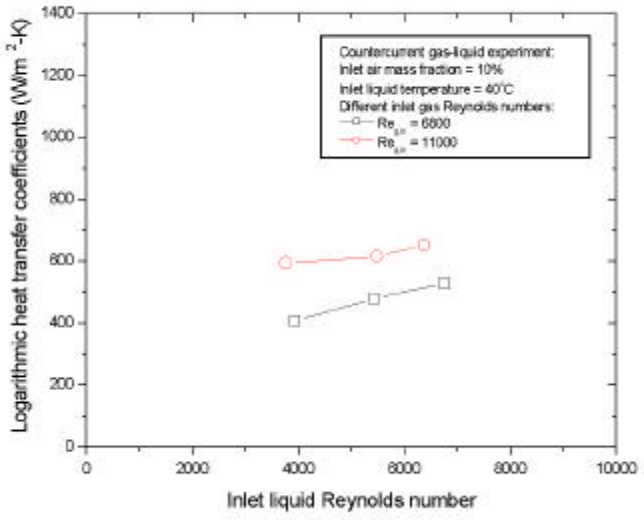

Figure 9. Effect of the inlet liquid Reynolds number on logarithmic heat transfer coefficient

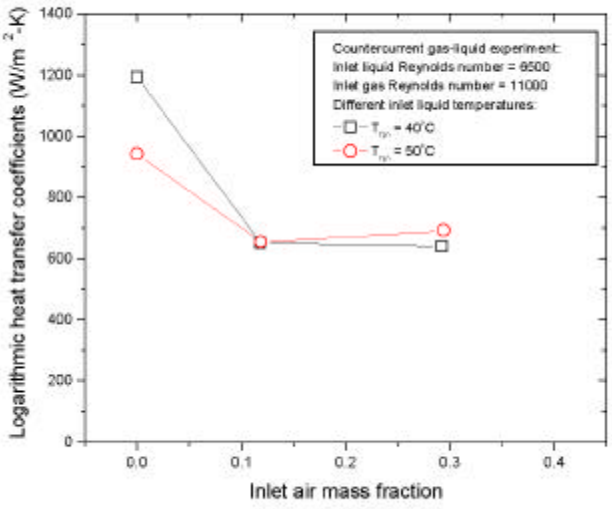

Figure 10. Effect of the inlet air mass fraction on logarithmic heat transfer coefficient

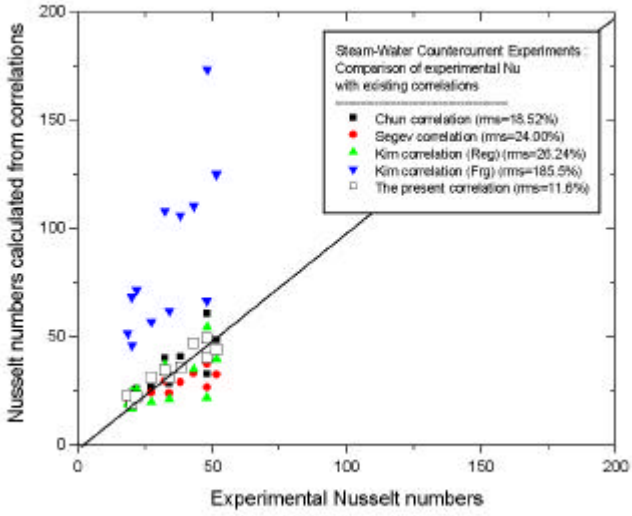

Figure 11. Comparison of Nusselt numbers estimated from the experimental data with those calculated from the present correlation and four existing correlations